Chemical Research in Toxicology

Article

pubs.acs.org/crt

Stability of *N*-Glycosidic Bond of (5′*S*)-8,5′-Cyclo-2′-deoxyguanosine

Rajat S. Das, Milinda Samaraweera, Martha Morton,[†] José A. Gascón, and Ashis K. Basu*

Department of Chemistry, University of Connecticut, Storrs, Connecticut 06269, United States

Supporting Information

ABSTRACT: 8,5′-Cyclopurine deoxynucleosides are unique tandem lesions containing an additional covalent bond between the base and the sugar. These mutagenic and genotoxic lesions are repaired only by nucleotide excision repair. The *N*-glycosidic (or C1′-N9) bond of 2′-deoxyguanosine (dG) derivatives is usually susceptible to acid hydrolysis, but even after cleavage of this bond of the cyclopurine lesions, the base would remain attached to the sugar. Here, the stability of the *N*-glycosidic bond and the products formed by formic acid hydrolysis of (5′*S*)-8,5′-cyclo-2′-deoxyguanosine (*S*-cdG) were investigated. For comparison, the stability of the *N*-glycosidic bond of 8,5′-cyclo-2′,5′-dideoxyguanosine (ddcdG), 8-methyl-2′-deoxyguanosine (8-Me-dG), 7,8-dihydro-8-oxo-2′-deoxyguanosine (8-Oxo-dG), and dG was also studied. In various acid conditions, *S*-cdG and ddcdG exhibited similar stability to hydrolysis. Likewise, 8-Me-dG and dG showed comparable stability, but the half-lives of the cyclic dG lesions were at least 5-fold higher than those of dG or 8-Me-dG. NMR studies were carried out to investigate the products formed after the cleavage of the C1′-N9 bond. 2-Deoxyribose generated α and β anomers of deoxyribopyranose and deoxyribopyranose oligomers following acid treatment. *S*-cdG gave α- and β-deoxyribopyranose linked guanine as the major products, but α and β anomers of deoxyribofuranose linked guanine and other products were also detected. The *N*-glycosidic bond of 8-Oxo-dG was found exceptionally stable in acid. Computational studies determined that both the protonation of the N7 atom and the rate constant in the bond breaking step control the overall kinetics of hydrolysis, but both varied for the molecules studied indicating a delicate balance between the two steps. Nevertheless, the computational approach successfully predicted the trend observed experimentally. For 8-Oxo-dG, the low pK_a of O[8] and N3 prevented appreciable protonation, making the free energy for *N*-glycosidic bond cleavage in the subsequent step very high.

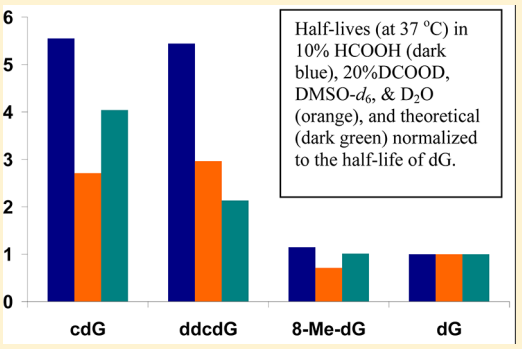

INTRODUCTION

The tandem DNA lesions, 8,5′-cyclopurine 2′-deoxynucleosides (cPDNs), formed by ionizing radiation and other processes that generate reactive oxygen species, are unique in that they contain damage to both the purine base and the 2′-deoxyribose sugar moiety.[1] These lesions exist as 5′*R* and 5′*S* diastereomers and have been detected in vitro and in vivo in DNA derived from many different cells and organisms.[2−4] Although these lesions were discovered in the 1960s,[5] they received more attention in recent years prompted by two reports in 2000 showing that in mammalian cells 8,5′-cyclo-2′deoxyadenosine (cdA) diastereomers are repaired by nucleotide excision repair (NER) and not by base excision repair.[6,7] However, a study in 2010 provided evidence for involvement of the DNA repair enzyme NEIL1 in NER of *R*-cdA and *S*-cdA in mice, although the mechanism remains unclear.[8] *R*-cdA is more efficiently repaired by NER than *S*-cdA, indicating that the stereochemistry of these lesions are important.[6] The cPDNs have been claimed to play a role in neurologic diseases in certain Xeroderma Pigmentosum patients with defects in NER.[9] It was also shown that *S*-cdA accumulates in vivo in genomic DNA of csb$^{-/-}$ mice, suggesting that this lesion may accumulate in Cockayne syndrome patients.[10] *S*-cdA has been reported to be a strong block of gene expression in Chinese hamster ovary and human cells.[7] It prevents the binding of TATA binding protein and strongly reduces transcription in vivo.[11] Both *R*-cdA and *S*-cdA block the elongation of a primer in vitro by mammalian DNA polymerase δ and T7 DNA polymerase,[6] whereas mammalian DNA polymerase η can bypass *R*-cdA but not *S*-cdA.[12] Recently, (5′*S*)-8,5′-cyclo-2′-deoxyguanosine (*S*-cdG) was shown to be significantly mutagenic in *Escherichia coli* inducing primarily *S*-cdG→A mutations.[13,14] The structures of oligodeoxynucleotide duplexes containing a site-specific *S*-cdG lesion placed opposite dC, dT, or dA in the complementary strand were obtained by a combination of solution NMR spectroscopy and molecular dynamics calculations.[15,16] These studies showed that the *S*-cdG deoxyribose is in the O4′-*exo* (west) pseudorotation in each pair. The Watson−Crick base pairing was conserved in the *S*-cdG·dC pair, whereas the *S*-cdG·dT pair adopts a wobble pairing. In contrast, no hydrogen bonding was observed for the *S*-cdG·dA pair, which differs in conformation from the dG·dA mismatch pair.

For many DNA lesions, structural changes of the purine or pyrimidine residue accompany destabilization of the *N*-glycosidic bond. The N7 position of guanine is the most nucleophilic site among the DNA bases, and 2′-deoxyguanosine

Received: July 3, 2012
Published: October 1, 2012

   dx.doi.org/10.1021/tx300302a | *Chem. Res. Toxicol.* 2012, 25, 2451−2461

(dG) is particularly susceptible to acid-catalyzed depurination.[17] The p*K*a of N7-protonated dG in DNA has been estimated to be between 2.5 and 3.0.[18] In low pH, therefore, S_N1 type hydrolysis occurs via protonation at the N7 position of dG followed by cleavage of the C1′-N9 bond. Theoretical studies show that for dG at neutral pH, the hydrolysis consists of two steps, but the Gibbs free energy barrier for the first step is very high.[19] By contrast, the N7-protonated dG follows a different two-step mechanism with a much lower Gibbs free energy barrier for the first step,[19,20] classified as $D_N + A_N$ reaction (or $D_N{}^*A_N$ where "*" indicates that a short-lived oxacarbenium ion is formed).[21] Because of the C8−C5′ covalent bond in cPDNs, it is anticipated that the purine and the deoxyribose will remain attached even after the cleavage of the C1′-N9 bond. The hydrolysis of the *N*-glycosidic bond of *S*-cdA has been shown to be ∼40-fold more stable than dA in acid,[22] but the chemical stability of the *N*-glycosidic bond of either *R*- or *S*-cdG is not known. Herein, we have investigated the stability of the *N*-glycosidic bond of *S*-cdG in comparison to dG and several analogues of *S*-cdG, including a cyclic analogue (ddcdG), an acyclic analogue (8-Me-dG), and 8-Oxo-dG (Chart 1). The products formed following hydrolysis of the C1′-N9 bond were also investigated.

Chart 1. Structures of the Compounds Used in This Study for *N*-Glycosidic Bond Cleavage: *S*-cdG, ddcdG, 8-Me-dG, 8-Oxo-dG, and dG

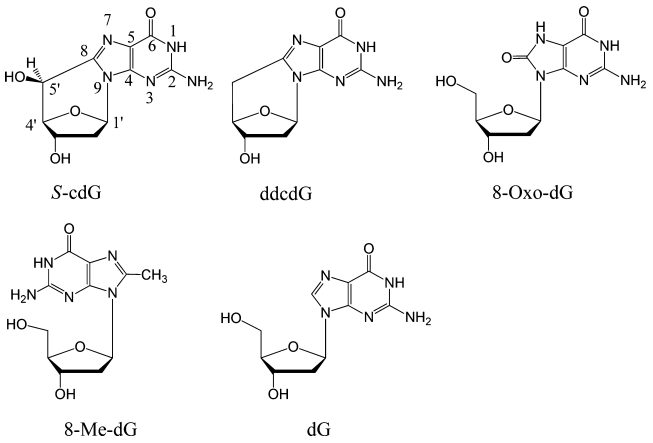

MATERIALS AND METHODS

S-cdG and ddcdG were synthesized and characterized as reported.[15,23] 8-Me-dG was prepared according to Kohda et al.[24] 8-Oxo-dG and dG were purchased from Berry and associates (Dexter, MI). Bulk solvents were purchased either from Sigma Aldrich (St. Louis, MO) or Fisher Scientific (Clifton, NJ). Deuterated solvents were purchased from Cambridge Isotope Laboratories (Andover, MA). Water used for this study was obtained from a Barnstead Nanopure System (Thermo Scientific, Dubuque, IA). All reagents used were of the highest purity available. The silica gel used for flash chromatography (40−63 μm) and gravitational column (63−200 μm) were purchased from Sorbent Technology (Norcross, GA). NMR data were analyzed using TOPSPIN software and referenced against a residual solvent peak. Mass spectral analyses were performed on a Qstar Elite mass spectrometer (Applied Biosystems, Carlsbad, CA) using collision-induced dissociation to detect the fragmentation pattern.

HPLC Analysis. HPLC analyses were performed on a reversed phase column (Synergi 4 μm Hydro-RP 80 Å LC Column 250 × 4.6 mm, Phenomenex, Torrance, CA) using a Waters 1525 HPLC system (Waters, Milford, MA) equipped with a diode-array detector (model 2996). A gradient elution program with 100% water to 15% acetonitrile with a flow rate of 1 mL/min in 20 min was used.

Formic Acid Hydrolysis. The acid hydrolysis was monitored either at regular intervals after treatment with a specific acid concentration, or the reaction time was kept constant, but the acid concentration was varied. For the time-course experiments, ∼3 nmol of samples were incubated in 10% (v/v) formic acid at 37 °C for various times, and an aliquot was neutralized with ice cold ammonia solution. To determine the effect of increasing acid concentration on *N*-glycosidic bond stability, ∼3 nmol of samples were incubated in various concentrations of formic acid for 4 h, and the reaction mixtures were neutralized with ice-cold ammonia. After drying, a known amount (1 nmol) of adenosine was added as internal standard to each sample, and the total volume was made up to 100 μL by adding water. The samples were injected on to a C18 analytical column. The amount of hydrolyzed product formed or the remaining nucleoside was measured by integrating the area under peak at 254 nm.

NMR Analysis. For dG and 8-Me-dG, NMR kinetic experiments were performed on a Bruker Avance III 400 MHz NMR spectrometer in 10% DMSO-d_6, 20% DCOOD and 70% D_2O. For ddcdG, the data including ^{13}C data were obtained through direct detection methods. The experiments to determine the acid decomposition products were run on a Bruker Avance I 400 MHz NMR spectrometer. Since the solubility of *S*-cdG in the above solvent mixture was poor, the spectra were recorded on a Varian Inova 600 MHz NMR spectrometer with a ^1H detect cold probe, and the ^{13}C data were acquired using indirect detection from the ^{13}C HSQC and HMBC. For a typical hydrolysis experiment, approximately 30 mM solution of the substrate was prepared in 600 μL of 20% DCOOD, 70% D_2O, and 10% D6-DMSO. This solution was immediately introduced into the spectrometer for kinetic studies, and the probe temperature was maintained at 37 °C. Because of the very poor solubility of *S*-cdG, the sample was prepared in a similar way, and the turbid solution was centrifuged at 14000 rpm for 2 min. The clear supernatant was used for the kinetic studies. The ratio of the products formed from 2-deoxyribose was determined from the integrals of the two deoxyribopyranose and the oligomer peaks from the C1′ protons between 4.5 and 5.5 ppm and from the C2′ protons between 1.4 and 2.5 ppm. Similarly, for ddcdG and *S*-cdG the integrals of the C2′ protons between 1.5 and 2.7 ppm were used.

Computational Methods. Geometry optimization of reactant and transition states were carried out with the quantum chemistry package Gaussian 09,[25] using density functional theory (DFT) with the B3LYP[26,27] functional and basis set 6-31++G(d,p). Solvent effects were taken into account using the polarized continuum model (PCM)[28] with water as an implicit solvent. Transition state structures were located using the synchronous transit-guided quasi-Newton method.[29] Harmonic vibrational frequencies were calculated for the stationary points. This frequency analysis was also used to calculate Gibbs free energies at 310.0 K, needed to determine activation free energy barriers and rate constants.

Protonation of the N7 atom in the nucleoside (Nu) induces the cleavage of the *N*-glycosidic bond followed by nucleophilic substitution of the formed oxacarbenium ion by water, leading to the corresponding products (Scheme 1).

Scheme 1

$$\mathrm{Nu} + \mathrm{H^+} \rightleftharpoons \mathrm{NuH^+} \xrightarrow[\mathrm{H_2O}]{k_2} \mathrm{NuOH} + \mathrm{H^+}$$

The nucleosides 8-Me-dG, dG, ddcdG, and *S*-cdG involve a rapid pre-equilibrium between the protonated and unprotonated states of N7 atom before the slow rate determining step (k_2), thus leading to an overall rate constant (k_{obs}) as follows:

$$k_{obs} = \frac{k_2}{10^{-pKa}}[H^+] = \frac{k_2}{K_a}[H^+] \quad (1)$$

where k_2 is the rate constant for the cleavage of the *N*-glycosidic bond (rate determining step), calculated according to the Eyring equation:

$$k_2 = \frac{k_B T}{h} e^{-\Delta^{\ddagger}G/RT} \quad (2)$$

where $\Delta^{\ddagger}G$ is the free energy of activation, k_BT is the thermal energy (T = 310.15 K), R is the gas constant, and h the Planck constant. The pK_a at the N7 position was calculated with the pK_a module in the quantum chemistry package Jaguar (Schrödinger, Inc.).[30] The half-life was computed as $t_{1/2} = 0.693/k_{obs}$. Equations 1 and 2 imply that, at constant k_2, the lower the pK_a, the more stable is the bond (larger $t_{1/2}$). Similarly, at constant pK_a, the lower k_2, the more stable is the bond.

RESULTS

***N*-Glycosidic Bond Cleavage of *S*-cdG.** To determine the identity of the products formed via cleavage of the *N*-glycosidic bond of *S*-cdG, we treated it with 10% formic acid at 37 °C and analyzed the products by reverse-phase HPLC. Figure 1 shows the HPLC chromatogram after 7 h of treatment, in which part of *S*-cdG (the 13.7 min peak) was converted to two other products, the first one eluting at 10.8 min followed by a small broad peak eluting at 11.7 min. We referred to the first 10.8 min peak as hydrolyzed cdG (hcdG). Mass spectral analysis of hcdG showed a mass ion of 284.1 Da, representing the protonated molecular ion (MH^+) of a H_2O (18 Da) addition product of *S*-cdG (*m/z* 266), as well as the sodium adduct ion (MNa^+) at 306 Da (Figure 2). Mass fragmentation of hcdG was analyzed by collision-induced dissociation (CID MS/MS), which exhibited ions at *m/z* 266, 248, and 230 owing to three consecutive water eliminations, plus 194 and 180 (Figure 2 inset). Since the mass of *S*-cdG is 266, the ion at *m/z* 180 originated from the base moiety plus the 5′-CHOH part of the sugar. The ion at *m/z* 194 is likely to be a fragment ion composed in addition to the base and 5′-CHOH, the 4′-CH (plus an H). Taken together, these data suggest that hcdG is the hydrolysis product of *S*-cdG. We considered it likely that the cleavage of the C1′-N9 bond followed by the addition of a water molecule generates hcdG, which is consistent with a stepwise formation of the oxacarbenium ion intermediate that undergoes nucleophilic attack by the water molecule in an S_N1 mechanism ($D_N{*}A_N$) (Scheme 2). The relative amount of the second broad peak at 11.7 min varied from one injection to another and, upon reinjection, it gave >95% of the first peak, hcdG, suggesting that it is one of the unstable intermediates.

When dG was incubated with acid under similar conditions, it was 77% converted to guanine in 2 h (when only 18% *S*-cdG

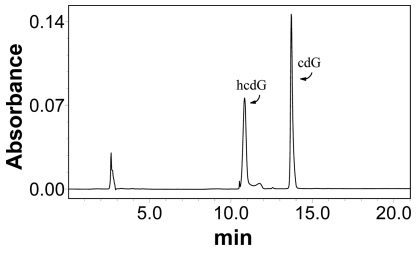

Figure 1. Reverse-phase HPLC profile of *S*-cdG following incubation with 10% formic acid at 37 °C for 7 h.

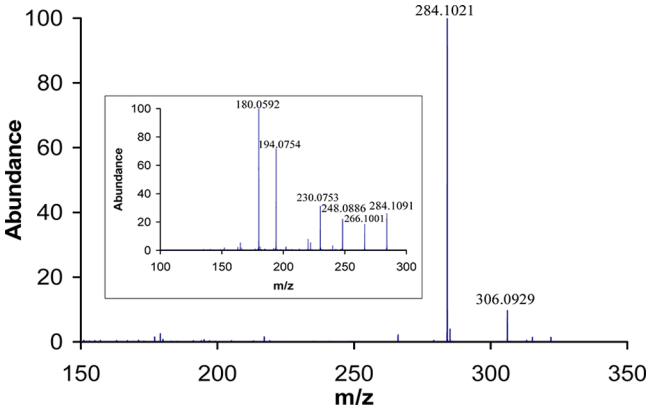

Figure 2. Mass spectrometry analysis of hcdG. MS-MS of 284.1 peak is shown in the inset.

Scheme 2. Postulated Mechanism of Acid-Catalyzed *N*-Glycosidic Bond Cleavage of *S*-cdG

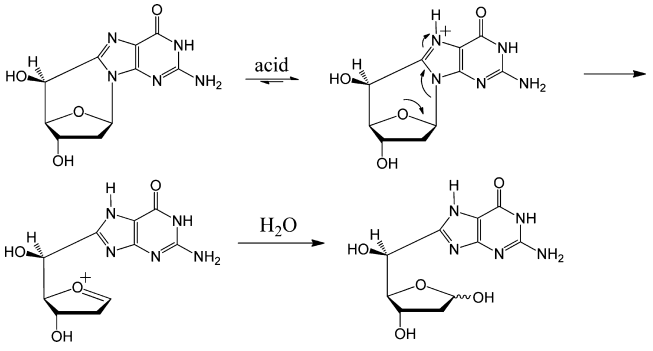

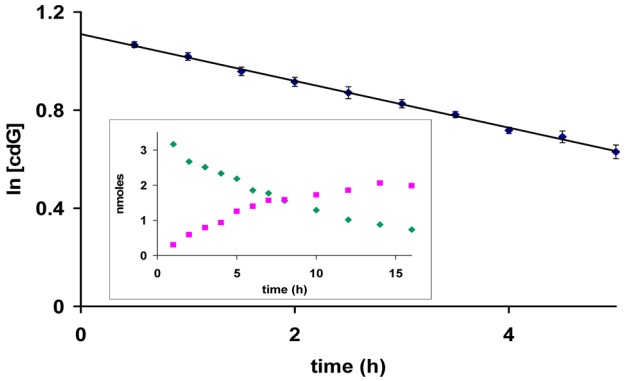

Figure 3. Kinetics of *N*-glycosidic bond cleavage of *S*-cdG in 10% formic acid at 37 °C monitored by HPLC. The inset shows the disappearance of the *S*-cdG peak (green diamonds) and appearance of the hcdG peak (pink squares) with time.

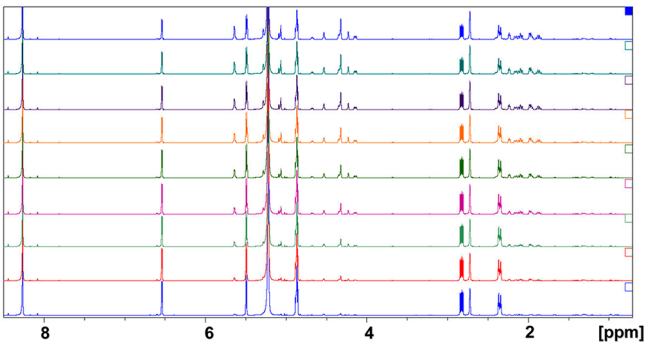

Figure 4. ^{1}H NMR time course analysis (shown here for the first two hours) (calibrated with the formic acid peak at 8.26 ppm) of *S*-cdG in 10% DMSO-d_6, 20% DCOOD, and 70% D_2O at 37 °C. The H-1′ peak (moved downfield to 6.52 ppm) was integrated to measure the loss of *S*-cdG. Starting from the bottom panel at zero time, spectra were taken every 15 min.

dx.doi.org/10.1021/tx300302a | *Chem. Res. Toxicol.* 2012, 25, 2451−2461

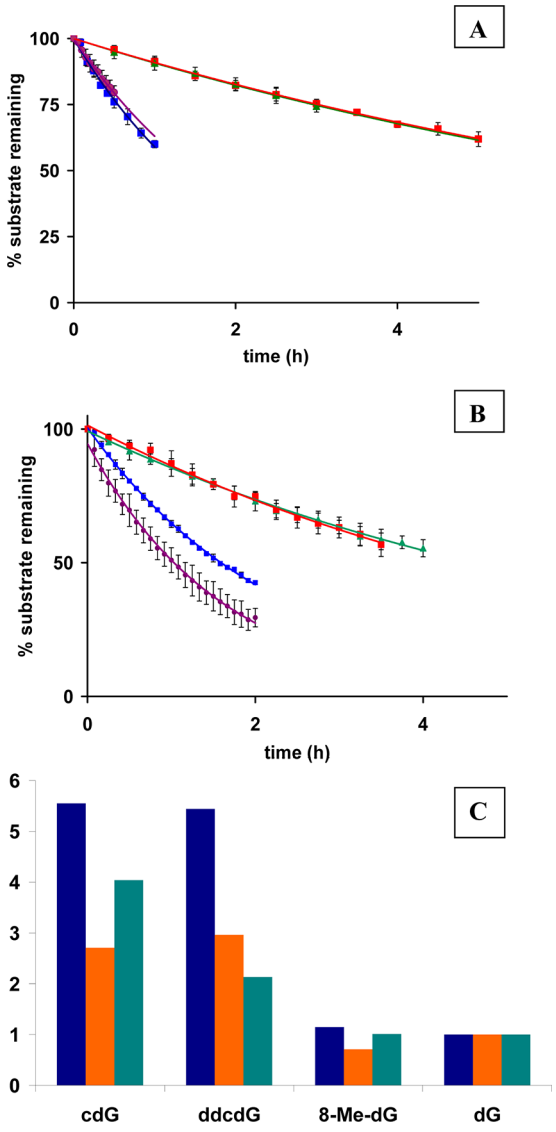

Figure 5. Comparison of the kinetics of *N*-glycosidic bond cleavage of *S*-cdG (red filled squares), ddcdG (green filled triangles), 8-Me-dG (purple filled circles), and dG (blue filled squares) in (A) 10% formic acid at 37 °C monitored by HPLC and (B) 20% DCOOD, 10% DMSO-d_6, and 70% D_2O at 37 °C monitored by ^{1}H NMR of the H-1′ peak. Each point represents at least three independent determinations. Their half-lives calculated from panel A (dark blue) and B (orange) and normalized to that of dG are shown in panel C. The half-lives determined by the computational study (Table 2) are also shown here in dark green.

was hydrolyzed), suggesting that *S*-cdG was significantly more resistant to acid hydrolysis. In order to further investigate the *N*-glycosidic bond stability of *S*-cdG, we compared the kinetics of cleavage of this cyclopurine nucleoside with 8,5′-cyclo-2′,5′-dideoxyguanosine (ddcdG), a cyclic analogue, and 8-methyl-2′-deoxyguanosine (8-Me-dG), an acyclic analogue of cdG (Chart 1). We selected these two compounds because, like *S*-cdG, each compound contains an sp^3-hybridized carbon attached to guanine-C8, but only ddcdG contains an additional ring like *S*-cdG. We also analyzed the *N*-glycosidic bond stability of dG and 8-Oxo-dG, the latter containing an oxygen substitution at guanine-C8. In one set of experiments, we monitored the *N*-glycosidic bond cleavage at 37 °C in 10% formic acid by reverse-phase HPLC. Figure 3 shows the kinetics of hydrolysis

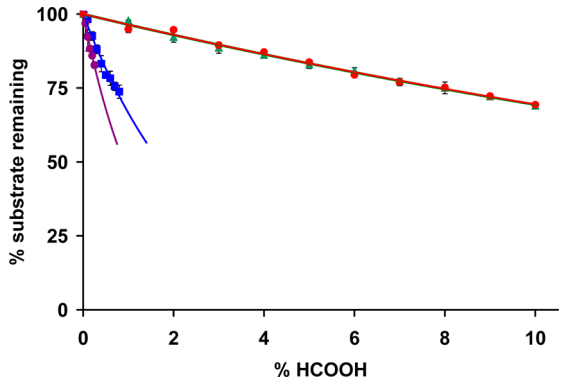

Figure 6. HPLC monitoring of *N*-glycosidic bond cleavage of *S*-cdG (red filled squares), ddcdG (green filled triangles), Me-dG (purple filled circles), and dG (blue filled squares) after 4 h of treatment at 37 °C with increasing concentrations of formic acid.

of *S*-cdG, including the time course of generation of the hcdG peak in the inset. The hydrolysis was also monitored by ^{1}H NMR (Figure 4), except that we used 20% DCOOD, 10% DMSO-d_6, and 70% D_2O due to the poor solubility of *S*-cdG in 10% deuterated formic acid. The kinetics of hydrolysis was followed by integrating the H-1′ peak area at 6.52 ppm since it became smaller as more substrate was hydrolyzed. When similar experiments were performed with dG, ddcdG, and 8-Me-dG, it was apparent that the hydrolysis of *S*-cdG was similar to that of ddcdG, whereas dG hydrolysis was comparable to 8-Me-dG (Figure 5). As shown in Figure 5A, in which reverse-phase HPLC monitoring was employed, and in Figure 5B, which utilized NMR monitoring of the intensity of H-1′ proton signal, the kinetics of hydrolysis of the four compounds followed an analogous trend, despite the differences in acid conditions. The half-lives ($t_{1/2}$) of the four compounds show a similar pattern (Figure 5C), also indicating that *S*-cdG hydrolysis was more than 5 times slower than dG. We also determined that 8-Oxo-dG was much more resistant to hydrolysis than the four other nucleosides evaluated here, in that >99% of 8-Oxo-dG was recovered after incubation in 10% formic acid for 7 days at 37 °C (data not shown). In another set of experiments, we varied the formic acid concentrations but analyzed the products in each case after a 4 h time interval (Figure 6). The concentration of formic acid needed to obtain 50% depurination of dG was 1.7% compared to 19% for *N*-glycosidic bond cleavage of *S*-cdG, whereas the same for ddcdG and 8-Me-dG were 18.9% and 0.9%, respectively. Again, the acid concentration needed to cause 50% hydrolysis of *S*-cdG was similar to that of ddcdG, whereas the same for 8-Me-dG and dG was comparable. However, compared to dG or 8-Me-dG a 10-fold acid higher concentration was needed to hydrolyze 50% *S*-cdG or ddcdG. On the basis of these three sets of experiments, we conclude that the *N*-glycosidic bond of *S*-cdG is 5−10-times more stable to acid hydrolysis than that of dG.

NMR Analysis of *N*-Glycosidic Bond Cleavage of *S*-cdG. In order to understand the products formed by acid hydrolysis of dG and dG derivatives, we followed the reaction of 2-deoxyribose in deuterated formic acid. After 24 h in 20% DCOOD, 10% DMSO-d_6, and 70% D_2O at 37 °C, both ^{13}C- and ^{1}H NMR indicated that 2-deoxyribose no longer had any detectable signal of the deoxyribofuranose form. As shown in Figure 7 (panels a and b), ^{1}H NMR indicated that four major products were generated from 2-deoxyribose, which included α-

dx.doi.org/10.1021/tx300302a | *Chem. Res. Toxicol.* 2012, 25, 2451−2461

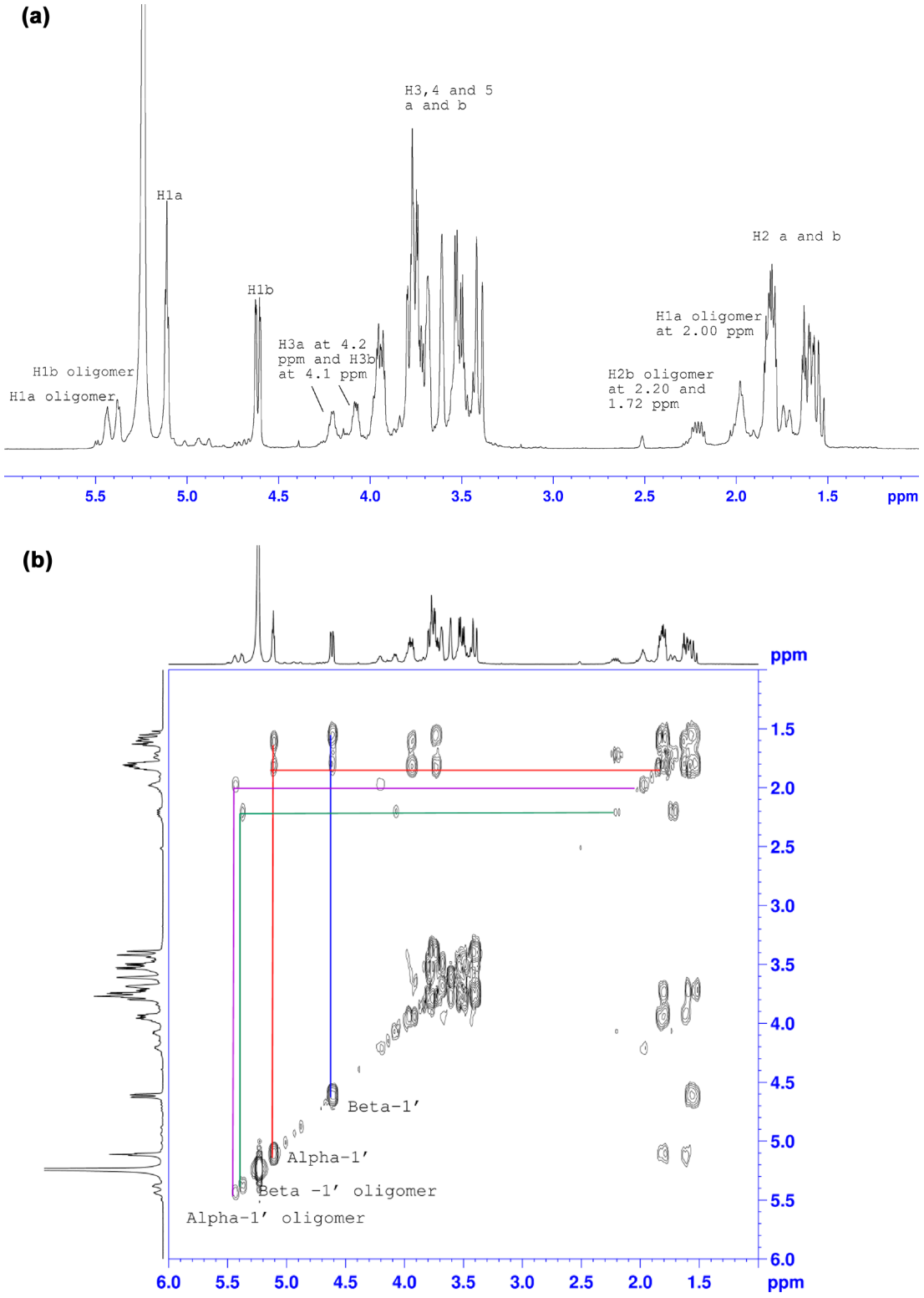

Figure 7. (a) ^{1}H NMR spectrum of 2-deoxyribose following acid hydrolysis in 20% deuterated formic acid. (b) COSY spectrum of the same, which leads to four products: α- and β-deoxyribopyranose (red and blue line, respectively), and oligomerized α- and β-deoxyribopyranose (purple and green line, respectively).

deoxyribopyranose (35%), β-deoxyribopyranose (30%), and two deoxyribopyranose oligomers (15% each) (Scheme 3). There also were other unidentified minor products. Additional details of the spectral data are provided in Table S1 (Supporting Information). Formic acid hydrolysis of dG and 8-Me-dG under similar conditions showed a nearly identical product profile, in addition to the heterocyclic base (data not shown). It is noteworthy that when DCOOD was replaced with DCl, extensive polymerization and degradation of the sugar took place, making the product profile difficult to analyze (data not shown).

dx.doi.org/10.1021/tx300302a | *Chem. Res. Toxicol.* 2012, 25, 2451−2461

Scheme 3. Postulated Mechanism of Formic Acid-Catalyzed Reaction of 2-Deoxyribose

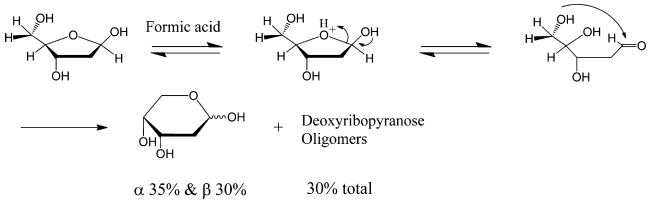

The ^{13}C chemical shift data of ddcdG in neutral and acidic conditions are shown in Table S2 in the Supporting Information. The upfield shift of −5.4 ppm at C5 and the downfield shift of 4.9 ppm at C8 on acidification with 10% deuterated formic acid suggest protonation of N7,[31,32] consistent with the general mechanism of *N*-glycosidic bond cleavage of dG derivatives as postulated in Scheme 2.

The ^{1}H NMR spectra of *S*-cdG in DMSO-d_6 is shown in Figure S1 in the Supporting Information. For *S*-cdG in acid, we could identify the guanine linked *α*- and *β*-deoxyribopyranose by C1′ chemical shift and H1′ coupling constants (Figure 8 and Table S3, Supporting Information). The guanine linked deoxyribofuranoses were identified by C1′ and C2′ chemical shifts. No oligomers were formed, presumably because of the steric effect of the attached guanine, but there was an unidentified product. We hypothesize this product to be a septanose derivative, formed via the attack of N7 or N9 of guanine to the aldehyde carbon of the ring-opened deoxyribose (Scheme 4). A septanose derivative was also detected in the reaction mixture of formic acid-hydrolyzed ddcdG, which cannot form the deoxyribopyranoses (Figure S2, Supporting Information). But definitive characterization of these compounds must await further investigation. The hydrolysis of 81% *S*-cdG generated the deoxyribopyranose derivatives as the major products (46%) with a small fraction (12%) of deoxyribofuranose derivatives and 23% other products, which included the suspected guanine linked septanose (Figure 8 and Scheme 4).

It is interesting to note that HPLC analyses of *S*-cdG hydrolysis gave one major peak, in addition to the unhydrolyzed starting material, as shown in Figure 1. Since the molecular mass of the various products shown in Scheme 4 is the same, we suspect that the 10.8 min peak in Figure 1 included all these different hcdG isomers. Our attempts to separate these molecules by HPLC using a variety of columns and conditions were unsuccessful, which may suggest that these isomeric deoxypyranoses, deoxyfuranoses, and other products remain in equilibrium.

Insights from the Computational Study. Computational studies are often a valuable complement to experimental observations. Accordingly, using a theoretical approach, we explored the effects of protonation of *S*-cdG in comparison to dG and the dG derivatives investigated here. Our goal was to compute the pK_a values of the protonated nucleosides as well as the activation energies and rate constants of the process represented in Scheme 1 so that their half-lives can be determined. Optimized geometries for reactants and their transition states were in agreement with structures previously reported.[19,33,34] In particular, in agreement with the literature data,[35,36] the minimum energy structure of dG and 8-Oxo-dG was in the anti conformation, whereas that of 8-Me-dG was measured in the syn conformation (Figure 9). Evidently, *S*-cdG and ddcdG are locked in the anti orientation (Figure 9). The pK_a of the protonated *S*-cdG was found lower than the other three nucleosides (Table 1). The computational prediction of the overall rate constants for the *N*-glycosidic bond cleavage (Table 1) allowed us to determine the factors for acid-catalyzed bond stability across all the dG derivatives studied. The experimentally observed order of stability and the ratio of half-lives of the nucleosides, using dG as a reference, showed a very good qualitative agreement with the calculated values (Table 2 and Figure 5C). According to eq 2, both the protonation of the N7 atom and the rate constant in the bond breaking step control the overall kinetics. Lower pK_a implies a lower number of protonated N7 molecules, thus diminishing the probability for the *N*-glycosidic bond cleaving. However, a higher activation barrier in this last process will also disfavor cleavage of the bond. Considering all these contributions in Table 1, it is clear that neither pK_a nor k_2 remain constant for the molecules studied. Thus, there appears to be a delicate balance between the two steps. Let us consider, for instance, the marked difference between the pK_a at the N7 position for *S*-cdG (2.7) and ddcdG (3.7). This difference alone affects the overall rate constant by an order of magnitude. Thus, in this case, it is the pK_a that is mostly the determining factor, although a higher k_2 of *S*-cdG relative to ddcdG partly counterbalanced its low pK_a. The origin of the more acidic proton in *S*-cdG is due to the unfavorable dipole−dipole interaction between the 5′-OH and the N7-H atom. When dG and 8-Me-dG, with almost identical stability, are compared, there appears to be a compensation of effects of almost equal magnitude. The slightly lower pK_a in dG tends to make the reaction slower by a factor of 2, while the actual water-mediated cleavage is faster by roughly a factor of 2.5. Finally, in the case of 8-Oxo-dG, stability is almost entirely determined by its inability to get protonated. Indeed, calculation of the pK_a at the O^8 position gives a negative value (not reported in Table 1). In this case, protonation can actually occur at the alternative N3 position. However, the previously reported pK_a value at N3 is also very small.[37] Thus, significant protonation cannot occur in weak acid conditions, making the free energy for cleavage in the next step very high. This result is consistent with 8-Oxo-dG having the maximum stability found experimentally relative to that of all other nucleosides studied in this work. Thus, we infer that the high stability of 8-Oxo-dG is largely dominated by the inability of the base to be protonated and not by the strength of the *N*-glycosidic bond.

Another relevant question is about the intrinsic effect of the cyclic structure of *S*-cdG. To answer this question, it is appropriate to select molecules that have a hydroxyl group at the 5′ position (i.e., *S*-cdG and dG). We proceeded by breaking the C5′-C8 bond in *S*-cdG and capping the two ends with hydrogen atoms. We carried out this by only permitting rotation of the CHOH group, while maintaining the C5′-C8 distance. This allowed us to estimate the effect of the cyclic form alone. As a result of this bond breaking, the pK_a changed from 2.7 to 3.1, which is very close to the pK_a value of the fully relaxed acyclic compound, dG (Table 1). This implies that the C5′-C8 bond is a necessary condition to make protonated N7 more acidic in *S*-cdG than in dG.

DISCUSSION

8,5′-Cyclopurine 2′-deoxynucleosides are biologically important DNA damages. Learning the chemical features of these molecules is critical for analyzing their biological effects. The

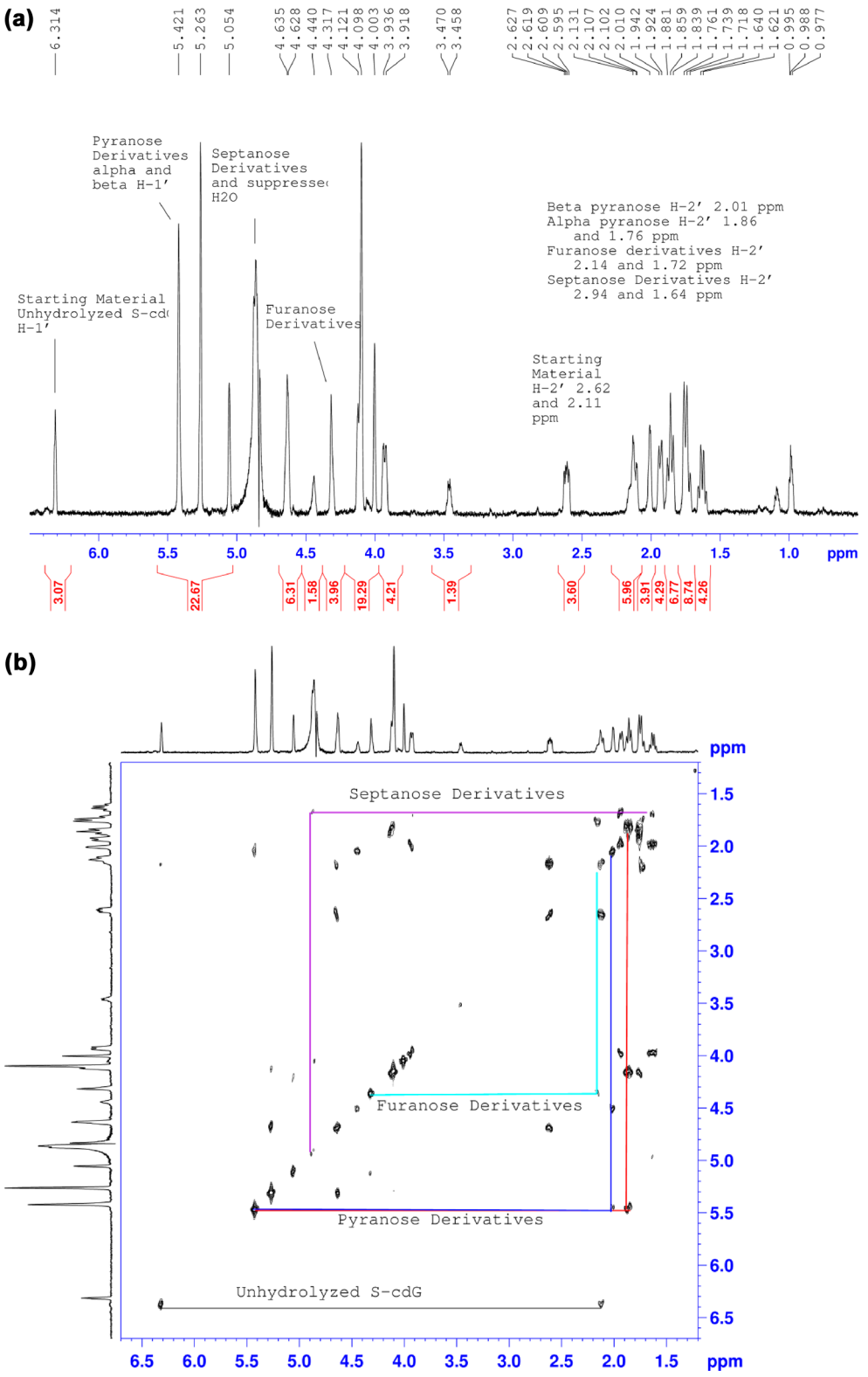

Figure 8. (a) ^{1}H NMR spectrum of *S*-cdG following acid hydrolysis in 20% deuterated formic acid. (b) COSY spectrum of the same, which leads to four products: α- and β-deoxyribopyranose (red and blue line), α- and β-deoxyribofuranose (green line), suspected septanose (fuchsia line), unhydrolyzed *S*-cdG (black line).

objective of this investigation on the chemical stability of the *N*-glycosidic bond of *S*-cdG was to provide a better understanding of this lesion. Using different acid conditions, we established that *S*-cdG and ddcdG were much more stable to acid than dG or 8-Me-dG. However, of the five compounds examined, 8-Oxo-dG was the most resistant to acid hydrolysis.

Role of the Six-Membered Ring and the Sugar Pucker of *S*-cdG. For nonenzymatic *N*-glycosidic bond cleavage, conformation changes in the sugar ring to promote favorable

dx.doi.org/10.1021/tx300302a | *Chem. Res. Toxicol.* 2012, 25, 2451−2461

Scheme 4. Formic Acid-Catalyzed Ring Opening and Rearrangement of *S*-cdG, According to the NMR Result[a]

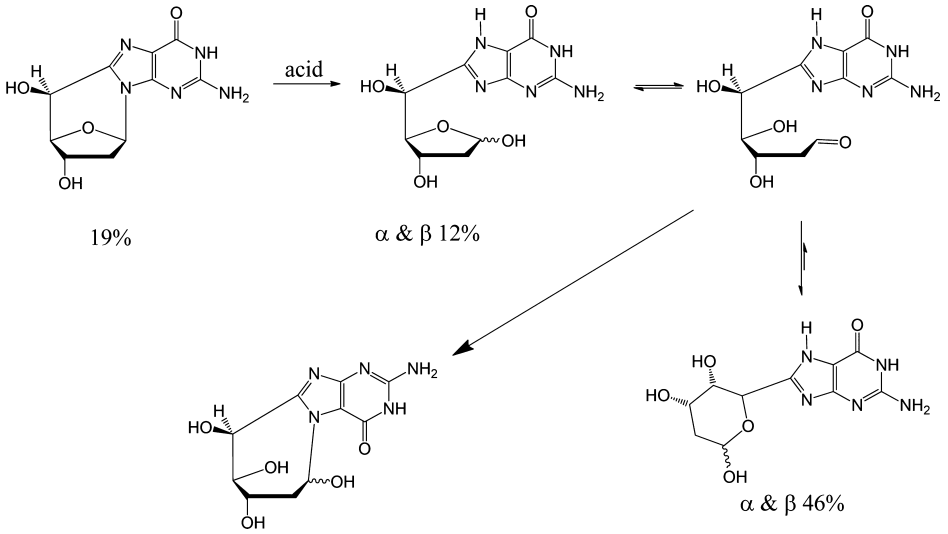

[a]The postulated structure of a septanose derivative is shown. These and other unidentified products have been detected at ∼23%.

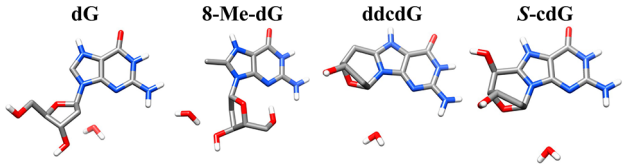

Figure 9. Computed minimum energy structures of dG (*anti*), 8-Me-dG (*syn*), ddcdG (*anti*), and *S*-cdG (*anti*) with a reactive water molecule.

Table 1. Computed Values of pK_a at the N7 Position, Activation Energies, and Rate Constants for Step 2 in the Reaction

molecule	pK_a	k_2	activation energy (kcal mol^{-1})
dG	3.2	98.2 × 10^{-4}	21.09
8-Me-dG	3.5	37.7 × 10^{-4}	21.52
ddcdG	3.7	12.0 × 10^{-4}	22.27
S-cdG	2.7	65.9 × 10^{-4}	21.30

Table 2. Ratio of the Half-Life of a Nucleoside to That of dG

molecule	ratio (experimentally, in 10% HCOOH monitored by HPLC)	ratio (experimentally, in 20% DCOOD, 10% DMSO-d_6 and 70% D_2O monitored by NMR)	ratio (theoretically)
dG	1.00	1.00	1.00
8-Me-dG	1.15	0.70	1.01
ddcdG	5.44	2.96	2.13
S-cdG	5.55	2.71	4.04

orbital interactions have been suggested to play a role.[38] Significantly higher *N*-glycosidic bond stability of *S*-cdG and ddcdG compared to dG and 8-Me-dG implies that the new six-membered bicyclic ring structure provides enhanced stability, which is consistent with an earlier investigation that reported *S*-cdA to be ∼40-fold more stable to acid than dA.[22] However, the computational studies indicate that such generalizations may not be valid and that the changes in each step of the pathway should be examined carefully as it is altered by the change in structure and conformation of the molecule. Two recent NMR investigations of *S*-cdG in DNA opposite three different partner bases revealed that in each case *S*-cdG deoxyribose shifts to the O4′-*exo* ("West") pseudorotation, which is likely maintained in the *S*-cdG nucleoside, as was reported for the *S*-cA riboside.[39] The NMR studies[15,16] showed that the six-membered ring C8-N9-C1′-O4′-C4′-C5′ adopts a half-chair conformation with the O4′ and C4′ puckered. The O4′-exo ("West") is considered an unstable conformer, owing to the axial orientation of the bulkier substituents. In this conformation, the lone pair of O4′ of the sugar seems suitably aligned with the C1′-N9 bond, which would allow the oxygen to stabilize the developing positive charge on C1′ during the bond breaking step. Therefore, a faster hydrolysis is expected, although the magnitude of this effect may be small.[40] In contrast, increased stability of the N9-C1′ bond for *S*-cdG was experimentally observed (Table 2). The computational study indicated that the ring formation in *S*-cdG results in an unfavorable dipole−dipole interaction between the 5′-OH and the N7-H atom. This interaction gives rise to increased acidity of the proton at N7 (Table 1), thereby enhancing the acid stability of the N9-C1′ bond. It is tempting to attribute this stability to the formation of the new six-membered bicyclic ring system since both *S*-cdG and ddcdG exhibit comparable stability to hydrolysis; however, the mechanism is more complex because N7-H of ddcdG is less acidic than any nucleoside examined in this study, except that a much lower rate constant for step 2 (k_2) in ddcdG hydrolysis relative to *S*-cdG (and others) counterbalanced its high pK_a.

Mechanistic Considerations and the Acid Hydrolysis Products. The ^{13}C chemical shift data in neutral and acidic conditions were consistent with the general mechanism of *N*-glycosidic bond cleavage of dG derivatives as postulated in Scheme 2. It has been well-established for more than 40 years that protonation gives rise to substantial acceleration to depurination of dG,[41] and theoretical studies show that the transition state energy is lowered by ∼10 kcal mol^{-1}.[42] In the D_N*A_N mechanism,[21] the N7 protonated dG leads to the generation of an oxacarbenium ion intermediate in the first step,[41,43,44] with a Gibbs free energy barrier of 19 kcal mol^{-1}.[19] In the second step, nucleophilic attack by the water molecule on the oxacarbenium ion to yield the final products is

dx.doi.org/10.1021/tx300302a | *Chem. Res. Toxicol.* 2012, 25, 2451−2461

considered a nearly barrier-less process.[19] For the cPDNs, previous DFT calculations show a large negative enthalpy for the *N*-glycosidic bond cleavage reactions of the protonated form.[45] Our calculations of the hydrolysis of this set of nucleosides, based on DFT with the B3LYP[26] functional and basis set 6-31++G(d,p), accurately predicted the trend observed experimentally. We also found exceptionally high stability of the *N*-glycosidic bond of 8-Oxo-dG in acid, which was attributed to its inability to protonate the base.

What Happens After the Cleavage of the C1′-N9 Bond? For abasic sites, after the water addition the mixture of cyclic hemiacetals is the predominant form, and the acyclic aldehyde form was estimated to be less than 1%.[46,47] However, to our knowledge, there are no reports on the type of products formed from ring-opened furanose sugars with a purine attached to it. To examine the products formed after the cleavage of C1′-N9 bond, we first analyzed the products generated from 2-deoxyribose under acid conditions used in the *S*-cdG hydrolysis. From the sugar, only α and β anomers of deoxyribopyranose and deoxyribopyranose oligomers were detected. With formic acid hydrolyzed *S*-cdG, α- and β-deoxyribopyranose linked guanine were the major products. However, instead of the oligomeric products found in the reaction mixture of 2-deoxyribose, *S*-cdG gave a fraction of the two anomers of deoxyribofuranose linked guanine and other cyclic products (Scheme 4). As noted by others,[47] the ring-opened aldehyde form was nearly undetectable. Oligomeric products were not detected in ddcdG hydrolysis as well. We believe that the steric effect of guanine at the 5′ position of the sugar prevented oligomerization in *S*-cdG and ddcdG, but for *S*-cdG, six-membered deoxyribopyranoses were the major products.

Biological Implications. Base excision repair proteins can accelerate the hydrolysis of the *N*-glycosidic bond in the range 10^7−10^{12}-fold.[40] Although a variety of mechanisms are known to operate, a prevalent mechanism employs a water molecule to attack the anomeric carbon (C1′) of the nucleotide. For the cPDNs, no DNA glycosylase activity was detected in mammalian cellular extracts,[6,7] but NEIL1 was suspected to be involved in the repair of cdA.[8] In a more recent in vitro work, it was found that seven repair proteins, including NEIL1, which repair oxidative DNA damage, do not directly interact with *S*-cdG or *S*-cdA.[48]

Increased *N*-glycosidic bond stability of *S*-cdG compared to dG excludes the possibility of spontaneous depurination of this lesion from DNA. Since base excision repair proteins cannot repair this damage, NER remains the only mechanism for its removal from DNA. It is therefore conceivable that in NER compromised cells, this highly mutagenic lesion may persist for a long time to exert its deleterious effects.

■ ASSOCIATED CONTENT

Ⓢ Supporting Information

Additional NMR data. This material is available free of charge via the Internet at http://pubs.acs.org.

■ AUTHOR INFORMATION

Corresponding Author

*Tel: 860-486-3965. Fax: 860-486-2981. E-mail: ashis.basu@uconn.edu.

Present Address

†Department of Chemistry, University of Nebraska, Lincoln, NE.

Funding

This work was supported by the National Institute of Environmental Health Sciences, NIH (grant ES013324). Upgrade of the 400 MHz NMR at the University of Connecticut Chemistry Department was supported by NSF through the NSF-CRIF program.

Notes

The authors declare no competing financial interest.

■ ABBREVIATIONS

cPDN, 8,5′-cyclopurine 2′-deoxynucleoside; *S*-cdG and *R*-cdG, (5′*S*)- and (5′*R*)-8,5′-cyclo-2′-deoxyguanosine, respectively; *S*-cdA and *R*-cdA, (5′*S*)- and (5′*R*)-8,5′-cyclo-2′-deoxyadenosine, respectively; ddcdG, 8,5′-cyclo-2′,5′-dideoxyguanosine; 8-Oxo-dG, 7,8-dihydro-8-oxo-2′-deoxyguanosine; 8-Me-dG, 8-methyl-2′-deoxyguanosine; 2-deoxyribose, 2-deoxy-D-*erythro*-pentose; NER, nucleotide excision repair; HSQC, heteronuclear single quantum coherence; HMBC, heteronuclear multiple bond correlation

■ REFERENCES

(1) Chatgilialoglu, C., Ferreri, C., and Terzidis, M. A. (2011) Purine 5′,8-cyclonucleoside lesions: chemistry and biology. *Chem. Soc. Rev. 40*, 1368−1382.

(2) Jaruga, P., and Dizdaroglu, M. (2008) 8,5′-Cyclopurine-2′-deoxynucleosides in DNA: mechanisms of formation, measurement, repair and biological effects. *DNA Repair 7*, 1413−1425.

(3) Jaruga, P., Xiao, Y., Nelson, B. C., and Dizdaroglu, M. (2009) Measurement of (5′R)- and (5′S)-8,5′-cyclo-2′-deoxyadenosines in DNA in vivo by liquid chromatography/isotope-dilution tandem mass spectrometry. *Biochem. Biophys. Res. Commun. 386*, 656−660.

(4) Dizdaroglu, M., Jaruga, P., and Rodriguez, H. (2001) Identification and quantification of 8,5′-cyclo-2′-deoxy-adenosine in DNA by liquid chromatography/ mass spectrometry. *Free Radical Biol. Med. 30*, 774−784.

(5) Keck, K. (1968) [Formation of cyclonucleotides during irradiation of aqueous solutions of purine nucleotides]. *Z. Naturforsch., B: Chem. Sci. 23*, 1034−1043.

(6) Kuraoka, I., Bender, C., Romieu, A., Cadet, J., Wood, R. D., and Lindahl, T. (2000) Removal of oxygen free-radical-induced 5′,8-purine cyclodeoxynucleosides from DNA by the nucleotide excision-repair pathway in human cells. *Proc. Natl. Acad. Sci. U.S.A. 97*, 3832−3837.

(7) Brooks, P. J., Wise, D. S., Berry, D. A., Kosmoski, J. V., Smerdon, M. J., Somers, R. L., Mackie, H., Spoonde, A. Y., Ackerman, E. J., Coleman, K., Tarone, R. E., and Robbins, J. H. (2000) The oxidative DNA lesion 8,5′-(S)-cyclo-2′-deoxyadenosine is repaired by the nucleotide excision repair pathway and blocks gene expression in mammalian cells. *J. Biol. Chem. 275*, 22355−22362.

(8) Jaruga, P., Xiao, Y., Vartanian, V., Lloyd, R. S., and Dizdaroglu, M. (2010) Evidence for the involvement of DNA repair enzyme NEIL1 in nucleotide excision repair of (5′R)- and (5′S)-8,5′-cyclo-2′-deoxy-adenosines. *Biochemistry 49*, 1053−1055.

(9) Brooks, P. J. (2008) The 8,5′-cyclopurine-2′-deoxynucleosides: candidate neurodegenerative DNA lesions in xeroderma pigmentosum, and unique probes of transcription and nucleotide excision repair. *DNA Repair 7*, 1168−1179.

(10) Kirkali, G., de Souza-Pinto, N. C., Jaruga, P., Bohr, V. A., and Dizdaroglu, M. (2009) Accumulation of (5′S)-8,5′-cyclo-2′-deoxy-adenosine in organs of Cockayne syndrome complementation group B gene knockout mice. *DNA Repair 8*, 274−278.

(11) Marietta, C., Gulam, H., and Brooks, P. J. (2002) A single 8,5′-cyclo-2′-deoxyadenosine lesion in a TATA box prevents binding of the

TATA binding protein and strongly reduces transcription in vivo. *DNA Repair 1*, 967−975.
(12) Kuraoka, I., Robins, P., Masutani, C., Hanaoka, F., Gasparutto, D., Cadet, J., Wood, R. D., and Lindahl, T. (2001) Oxygen free radical damage to DNA. Translesion synthesis by human DNA polymerase eta and resistance to exonuclease action at cyclopurine deoxynucleoside residues. *J. Biol. Chem. 276*, 49283−49288.
(13) Jasti, V. P., Das, R. S., Hilton, B. A., Weerasooriya, S., Zou, Y., and Basu, A. K. (2011) 5′S)-8,5′-cyclo-2′-deoxyguanosine is a strong block to replication, a potent pol V-dependent mutagenic lesion, and is inefficiently repaired in *Escherichia coli*. *Biochemistry 50*, 3862−3865.
(14) Yuan, B., Wang, J., Cao, H., Sun, R., and Wang, Y. (2011) High-throughput analysis of the mutagenic and cytotoxic properties of DNA lesions by next-generation sequencing. *Nucleic Acids Res. 39*, 5945−5954.
(15) Huang, H., Das, R. S., Basu, A. K., and Stone, M. P. (2011) Structure of (5′S)-8,5′-cyclo-2′-deoxyguanosine in DNA. *J. Am. Chem. Soc. 133*, 20357−20368.
(16) Huang, H., Das, R. S., Basu, A. K., and Stone, M. P. (2012) Structures of (5′S)-8,5′-cyclo-2′-deoxyguanosine mismatched with dA or dT. *Chem. Res. Toxicol. 25*, 478−490.
(17) Pullman, A., and Pullman, B. (1981) Molecular electrostatic potential of the nucleic acids. *Q. Rev. Biophys. 14*, 289−380.
(18) Suzuki, T., Ohsumi, S., and Makino, K. (1994) Mechanistic studies on depurination and apurinic site chain breakage in oligodeoxyribonucleotides. *Nucleic Acids Res. 22*, 4997−5003.
(19) Rios-Font, R., Rodriguez-Santiago, L., Bertran, J., and Sodupe, M. (2007) Influence of N7 protonation on the mechanism of the N-glycosidic bond hydrolysis in 2 ′-deoxyguanosine. A theoretical study. *J. Phys. Chem. B 111*, 6071−6077.
(20) Przybylski, J. L., and Wetmore, S. D. (2010) Modeling the dissociative hydrolysis of the natural DNA nucleosides. *J. Phys. Chem. B 114*, 1104−1113.
(21) Guthrie, R. D., and Jencks, W. P. (1989) IUPAC recommendations for the representation of reaction-mechanisms. *Acc. Chem. Res. 22*, 343−349.
(22) Theruvathu, J. A., Jaruga, P., Dizdaroglu, M., and Brooks, P. J. (2007) The oxidatively induced DNA lesions 8,5′-cyclo-2′-deoxyadenosine and 8-hydroxy-2′-deoxyadenosine are strongly resistant to acid-induced hydrolysis of the glycosidic bond. *Mech. Ageing Dev. 128*, 494−502.
(23) Romieu, A., Gasparutto, D., and Cadet, J. (1999) Synthesis and characterization of oligonucleotides containing 5′,8-cyclopurine 2′-deoxyribonucleosides: (5′R)-5′,8-cyclo-2′-deoxyadenosine, (5′S)-5′,8-cyclo-2′-deoxyguanosine, and (5′R)-5′,8-cyclo-2′-deoxyguanosine. *Chem. Res. Toxicol. 12*, 412−421.
(24) Kohda, K., Tsunomoto, H., Minoura, Y., Tanabe, K., and Shibutani, S. (1996) Synthesis, miscoding specificity, and thermodynamic stability of oligodeoxynucleotide containing 8-methyl-2′-deoxyguanosine. *Chem. Res. Toxicol. 9*, 1278−1284.
(25) Frisch, M. J., Trucks, G. W., Schlegel, H. B., Scuseria, G. E., Robb, M. A., Cheeseman, J. R., Scalmani, G., Barone, V., Mennucci, B., Petersson, G. A., Nakatsuji, H., Caricato, M., Li, X., Hratchian, H. P., Izmaylov, A. F., Bloino, J., Zheng, G., Sonnenberg, J. L., Hada, M., Ehara, M., Toyota, K., Fukuda, R., Hasegawa, J., Ishida, M., Nakajima, T., Honda, Y., Kitao, O., Nakai, H., Vreven, T., Montgomery, J. A., Jr., Peralta, J. E., Ogliaro, F., Bearpark, M., Heyd, J. J., Brothers, E., Kudin, K. N., Staroverov, V. N., Kobayashi, R., Normand, J., Raghavachari, K., Rendell, A., Burant, J. C., Iyengar, S. S., Tomasi, J., Cossi, M., Rega, N., Millam, J. M., Klene, M., Knox, J. E., Cross, J. B., Bakken, V., Adamo, C., Jaramillo, J., Gomperts, R., Stratmann, R. E., Yazyev, O., Austin, A. J., Cammi, R., Pomelli, C., Ochterski, J. W., Martin, R. L., Morokuma, K., Zakrzewski, V. G., Voth, G. A., Salvador, P., Dannenberg, J. J., Dapprich, S., Daniels, A. D., Farkas, Ö., Foresman, J. B., Ortiz, J. V., Cioslowski, J., and Fox, D. J. (2009) *Gaussian 09*, Gaussian Inc., Wallingford, CT.
(26) Becke, A. D. (1993) Density-functional thermochemistry 0.3. The role of exact exchange. *J. Chem. Phys. 98*, 5648−5652.
(27) Lee, C. T., Yang, W. T., and Parr, R. G. (1988) Development of the Colle-Salvetti correlation-energy formula into a functional of the electron-density. *Phys. Rev. B 37*, 785−789.
(28) Cossi, M., Barone, V., Cammi, R., and Tomasi, J. (1996) Ab initio study of solvated molecules: A new implementation of the polarizable continuum model. *Chem. Phys. Lett. 255*, 327−335.
(29) Peng, C. Y., and Schlegel, H. B. (1993) Combining synchronous transit and quasi-Newton methods to find transition-states. *Israel J. Chem 33*, 449−454.
(30) *Jaguar* (2011) Schrödinger LLC, New York.
(31) Schindler, M. (1988) Magnetic-properties in terms of localized quantities 0.9. The DNA bases and the protonation of adenine. *J. Am. Chem. Soc. 110*, 6623−6630.
(32) Seckarova, P., Marek, R., Malinakova, K., Kolehmainen, E., Hockova, D., Hocek, M., and Sklenar, V. (2004) Direct determination of tautomerism in purine derivatives by low-temperature NMR spectroscopy. *Tetrahedron Lett. 45*, 6259−6263.
(33) Zheng, Y., Xue, Y., and Yan, S. G. (2008) The effects of oxidation and protonation on the N-glycosidic bond stability of 8-oxo-2 ′-deoxyguanosine: DFT study. *J. Mol. Struct.-Theochem. 860*, 52−57.
(34) Greisch, J. F., Leyh, B., and De Pauw, E. (2009) Collision induced dissociation of deuterium enriched protonated 2′-deoxyguanosine. *Eur. Phys. J. D 51*, 89−96.
(35) Lipscomb, L. A., Peek, M. E., Morningstar, M. L., Verghis, S. M., Miller, E. M., Rich, A., Essigmann, J. M., and Williams, L. D. (1995) X-ray structure of a DNA decamer containing 7,8-dihydro-8-oxoguanine. *Proc. Natl. Acad. Sci. U.S.A. 92*, 719−723.
(36) Xu, Y., Ikeda, R., and Sugiyama, H. (2003) 8-Methylguanosine: a powerful Z-DNA stabilizer. *J. Am. Chem. Soc. 125*, 13519−13524.
(37) Jang, Y. H., Goddard, W. A., 3rd, Noyes, K. T., Sowers, L. C., Hwang, S., and Chung, D. S. (2002) First principles calculations of the tautomers and pK(a) values of 8-oxoguanine: implications for mutagenicity and repair. *Chem. Res. Toxicol. 15*, 1023−1035.
(38) Gorenstein, D. G. (1987) Stereoelectronic effects in biomolecules. *Chem. Rev. 87*, 1047−1077.
(39) Haromy, T. P., Raleigh, J., and Sundaralingam, M. (1980) Enzyme-bound conformations of nucleotide substrates. X-ray structure and absolute configuration of 8,5′-cycloadenosine monohydrate. *Biochemistry 19*, 1718−1722.
(40) Stivers, J. T., and Jiang, Y. L. (2003) A mechanistic perspective on the chemistry of DNA repair glycosylases. *Chem. Rev. 103*, 2729−2759.
(41) Zoltewicz, J. A., Clark, D. F., Sharpless, T. W., and Grahe, G. (1970) Kinetics and mechanism of the acid-catalyzed hydrolysis of some purine nucleosides. *J. Am. Chem. Soc. 92*, 1741−1749.
(42) Baik, M. H., Friesner, R. A., and Lippard, S. J. (2002) Theoretical study on the stability of N-glycosyl bonds: why does N7-platination not promote depurination? *J. Am. Chem. Soc. 124*, 4495−4503.
(43) Hevesi, L., Wolfson-Davidson, E., Nagy, J. B., Nagy, O. B., and Bruylants, A. (1972) Contribution to the mechanism of the acid-catalyzed hydrolysis of purine nucleosides. *J. Am. Chem. Soc. 94*, 4715−4720.
(44) Kampf, G., Kapinos, L. E., Griesser, R., Lippert, B., and Sigel, H. (2002) Comparison of the acid-base properties of purine derivatives in aqueous solution. Determination of intrinsic proton affinities of various basic sites. *J. Chem. Soc. Perkin Trans. 2*, 1320−1327.
(45) Karwowski, B. T. (2010) The difference in stability between 5 ′ R and 5 ′ S diastereomers of 5 ′,8-cyclopurine-2 ′-deoxynucleosides. DFT study in gaseous and aqueous phase. *Cent. Eur. J. Chem. 8*, 134−141.
(46) Wilde, J. A., Bolton, P. H., Mazumder, A., Manoharan, M., and Gerlt, J. A. (1989) Characterization of the equilibrating forms of the aldehydic abasic site in duplex DNA by 17O-NMR. *J. Am. Chem. Soc. 111*, 1894−1896.
(47) Pierce, J., Serianni, A. S., and Barker, R. (1985) Anomerization of furanose sugars and sugar phosphates. *J. Am. Chem. Soc. 107*, 2448−2456.

(48) Pande, P., Das, R. S., Sheppard, C., Kow, Y. W., and Basu, A. K. (2012) Repair efficiency of (5′S)-8,5′-cyclo-2′-deoxyguanosine and (5′S)-8,5′-cyclo-2′-deoxyadenosine depends on the complementary base. *DNA Repair*, in press.